Supplementary Materials for "Ultra-High-Brightness and attosecond-long electron beams with the Laser Wake Field Acceleration"

Paolo Tomassini[1,*], Federico Avella[2], Nasr A. M. Hafz[3], Luca Labate[2], Vojtěch Horný[1], Szabolcs Tóth[3], Domenico Doria[1], and Leonida A. Gizzi[2]

[1]Extreme Light Infrastructure - Nuclear Physics, IFIN-HH, 30 Reactorului Street, 077125 Magurele, Romania
[2]Intense Laser Irradiation Laboratory, National Institute of Optics, CNR, 56124 Pisa, Italy
[3]The Extreme Light Infrastructure ERIC, ALPS Facility, Wolfgang Sandner Utca 3, H-6728 Szeged, Hungary
[*]paolo.tomassini@eli-np.ro

ABSTRACT

Additional materials about the dimensioning of the frequency-tripling setup, field ionization extracted electron beam properties the expected minimum achievable emittance are shown here.

Ionization pulse generation and focusing

The generation of ultrashort pulses in third harmonics is generally obtained with two crystals operating a Second Harmonic Generation (SHG) and a Third Harmonic Generation (THG) (see *e.g.*[1]). In order to predict the parameters and efficiency of the third-harmonic generation, a 3D numerical code[2,3] was used to simulate the SHG and the THG. The code includes dispersion, diffraction effects and crystal anisotropy. Therefore, temporal walk-off due to group velocity mismatch is taken into account which is the most important aspect during second- and third-harmonic generation of ultrashort pulses. The layout of the current frequency-tripling setup, consisting of a 300 µm thick Type I LBO crystal and a 70 µm thick Type I BBO crystal, is shown in Fig. 1-a). The peak intensities on the LBO and BBO crystals are 0.8 TW/cm² and 1 TW/cm², respectively. These intensity levels remain below the damage thresholds of the crystals at the current sub-30 fs pulse durations. According to the numerical results reported in Fig. 1-b,c), with a BBO thickness of 70 μm the converted pulse energy is exceeding 66 mJ and the temporal duration FWHM is below 30 fs.

The 66 mJ, 30 fs long pulse in III harmonics is subsequently expanded in diameter with a reflective telescope towards the second parabola having a diameter of 6 cm. As shown in Fig. 1-d) in the Main document, the positioning of the ionization pulse right behind the driver pulse, with collinear directions and close focal points, is obtained with a dedicated parabola and an holed mirror (which is equivalent to the usage of an holed parabola). In either ways, the long-focal F/38 "driver" parabola and the short-focal F/13 "ionization" parabola share the same axis, while the focal points are very close, within a mm scale. The hole-diameter is designed so as to assure the passage of the whole driver pulse train through it, with a beam fluency on the parabola/mirror well below the damaging threshold set to 0.2 J/cm^2 for a 25 fs long pulse. As it is apparent in panels a) and b) of Fig. 2

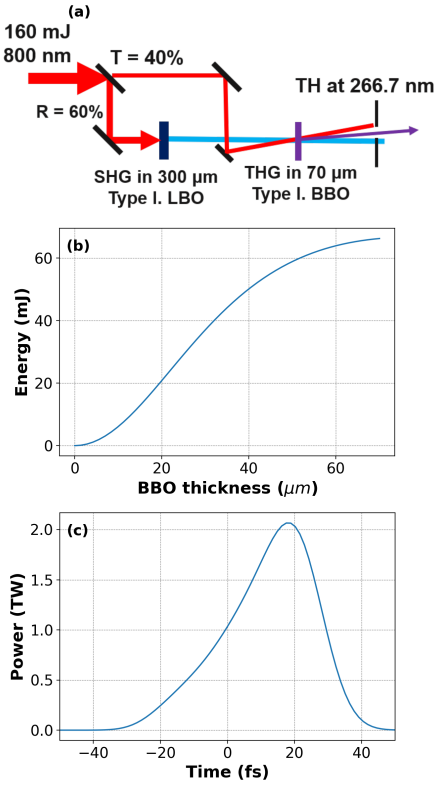

Figure 1. a) Proposed setup for third-harmonic generation (THG). According to simulations the optimal splitting ratio between SH and TH arms is 60:40, respectively. b) Energy of TH as a function BBO thickness. c) Temporal shape of the generated TH.

where numerical solutions of the propagation of the driver beams after the reflection upon the F/38 driver parabola and up to the ionization parabola (105 cm from the focal point) are reported, a hole of diameter 1.5 cm assures the whole driver beam propagation through the hole and a maximum fluence on the ionization parabola below $10^{-2} J/cm^2$. Panels c) and d) in Fig.2 show the ionization pulse distributions on the F/13 holed parabola and on the focal plane, respectively, unveiling that ionization pulses can be focused down the requested waist of $w_{0;i} = 3.7 \mu m$ reaching and intensity in excess of $5.7 \times 10^{18} W/cm^2$, above the requested value of $2.8 \times 10^{18} W/cm^2$ needed for the efficient extraction of the electrons from the dopant.

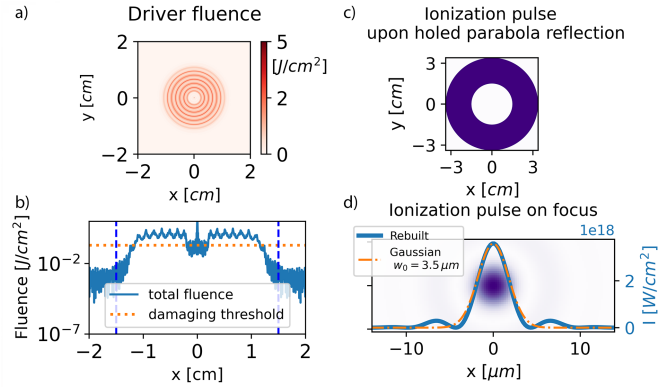

Figure 2. Delivering of the ionization pulse in a collinear direction with the driver train. The ionization pulse is made collinear with the driver train by using an holed F/13 parabola (or a parabola followed by an holed mirror), where the driver train from the F/38 parabola propagates into. a) The fluency of the driver train at the plane where the ionization pulse focusing parabola is placed and b) the vertical line-out at x=0 of the fluency, showing that with a hole having radius of 1.5 cm the whole of the driver beam propagates into the hole and fluence on the parabola is at least one order of magnitude below the damage threshold. c) The intensity distribution of the ionization pulse on the holed parabola and d) the ionization pulse focal spot assuming negligible aberrations, showing that the focusing system is capable of generating ionization pulses with an equivalent waist of about 3.5 μm and intensities exceeding $3.5 \times 10^{18} W/cm^2$.

Minimum achievable emittance scan

To numerically evaluate the minimum achievable emittance (see *Materials and Methods* of the main document), a scan around the ionization pulse working point of the whole beam size and momentum was obtained through the detailed model in[4] which includes saturation effects, complemented with the evaluation along the longitudinal ionization pulse focusing/defocusing around its focus point. Fig. 3-a) shows the dependence of the normalized emittance right after the pulse slippage on the ionization pulse amplitude. The model (diamonds in dash-dot line) is well matched with the results

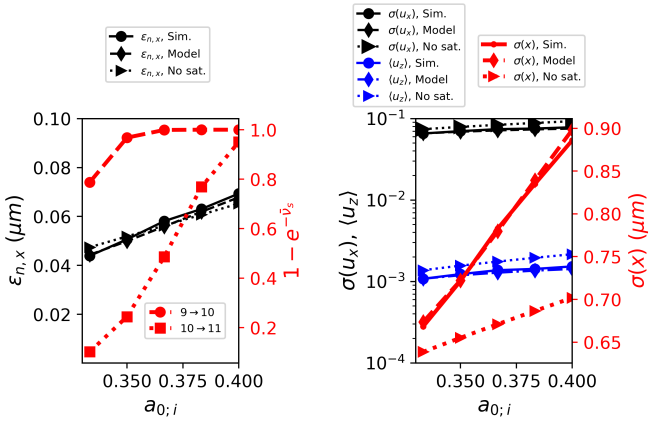

Figure 3. Scan on the ionization pulse amplitude of the whole beam residual momenta and transverse size after the ionization pulse passage. Data obtained by simulation (circles and full lines), the model which included saturation effects (diamonds in dash-dot lines) and, for comparison, the model which ruled out saturation effecs (triangles in dot lines). Left panel: normalized emittance scan. The right axis (in red) shows the fraction of extracted electrons for the two active $Ar^{9+\to10+}$ and $Ar^{10+\to11+}$. Right panel: *rms* transverse (black) and average longitudinal (blue) residual momenta. The right axis (in red) shows the *rms* transverse size scan.

obtained by Monte Carlo Simulations. The right (red) axis shows the fraction $1 - e^{-\bar{\nu}_s}$ of the electrons extracted on axis and near the pulse focus for both the active processes, thus confirming that the $Ar^{9+\to10+}$ is completely saturated around the working point $a_{0;i} = 0.38$. In Fig. 3-b) the scan of the momenta and transverse size on $a_{0;i}$ is shown. There, the saturation effects are visible, as both the momenta and the size from the simulations and from the full model differ significantly from those from the model which is ruling out the saturation effects (triangles in dot lines).

References

1. Fan-Chiang, L. *et al.* Third harmonic generation for two-color ionization injection in laser-plasma accelerators. In *2022 IEEE Advanced Accelerator Concepts Workshop (AAC)*, 1–3 (IEEE, 2022).
2. Andrianov, A. *et al.* Computationally efficient method for Fourier transform of highly chirped pulses for laser and parametric amplifier modeling. *Optics Express* **24**, 25974–25982, DOI: 10.1364/OE.24.025974 (2016).
3. Toth, S. *Optimization of high peak power few-cycle optical parametric chirped pulse amplifier systems*. Ph.D. thesis, University of Szeged (2021).
4. Tomassini, P., Massimo, F., Labate, L. & Gizzi, L. A. Accurate electron beam phase-space theory for ionization-injection schemes driven by laser pulses. *High Power Laser Science and Engineering* **10**, e15 (2022).